Organic Electronics 68 (2019) 50–55

Contents lists available at ScienceDirect

Organic Electronics

journal homepage: www.elsevier.com/locate/orgel

The effect of alkylthio substituents on the photovoltaic properties of conjugated polymers

Yi Li[a], Yuancong Zhong[a], Huanxiang Jiang[b], Thomas Rath[c], Qian Wang[b], Heike M.A. Ehmann[d], Gregor Trimmel[c], Shuguang Wen[b,**], Yong Zhang[a,*], Renqiang Yang[b]

[a] Institute of Optoelectronic Materials and Technology, South China Normal University, Guangzhou, 510631, China
[b] CAS Key Laboratory of Bio-based Materials, Qingdao Institute of Bioenergy and Bioprocess Technology, Chinese Academy of Sciences, Qingdao, 266101, China
[c] Institute for Chemistry and Technology of Materials (ICTM), NAWI Graz, Graz University of Technology, Stremayrgasse 9, 8010, Graz, Austria
[d] Anton Paar GmbH, Graz, Austria

ARTICLE INFO

Keywords:
Polymer solar cells
Alkylthio side chain
Non-covalent interaction
Conjugated polymer
Power conversion efficiency

ABSTRACT

Alkylthio groups are effectively utilized in molecule design to improve the performance of polymer solar cells (PSCs). In this study, two conjugated polymers, P1 and P2, were designed and synthesized with alkyl and alkylthio side chains substituted on thiophene as π bridges, respectively. Owing to the twist of the backbone induced by the steric hindrance of the hexyl side chains, polymer P1 shows a low power conversion efficiency (PCE) of 2.83% in PSC devices with $PC_{71}BM$ as acceptor and a low hole mobility of $1.85 \times 10^{-5}\,cm^2\,V^{-1}\,s^{-1}$ in the blend film. In contrast to the steric hindrance of the alkyl side chain, the alkylthio side chain can form S···S non-covalent interaction with an adjacent thiophene to maintain the molecular planarity and strengthen intermolecular interaction, which is designed in polymer P2 to improve the photovoltaic performance. As a result, the P2-based devices exhibit a higher PCE of 6.15% with an open-circuit voltage (V_{OC}) of 0.71 V, a short-circuit current (J_{SC}) of 14.55 mA cm^{-2} and a fill factor (FF) of 59.5%. The hole mobility is also increased to $2.20 \times 10^{-4}\,cm^2\,V^{-1}\,s^{-1}$. Our results demonstrate that introducing S···S non-covalent interaction into conjugated polymers could be a useful strategy for building high performance photovoltaic materials.

1. Introduction

In the past few years, great attention has been paid to the development of polymer solar cells (PSCs) owing to their merits such as light weight, low cost and easy fabrication [1–9]. In the bulk-heterojunction (BHJ) structure of PSCs, the photoactive layer, consisting of electron donor and acceptor materials, is the key part of PSCs, which absorbs photons, generates and dissociates excitons, and transfers charge-carries [10]. The π bridge, as a connection between the donor and acceptor moiety, has a significant effect on maintaining the molecular planarity in D-A type conjugated polymers [11–14]. However, the modification of the π bridge usually has the tendency to twist the polymer's backbone. Hence, a strategy to modify the π bridge while maintaining the planarity of polymer's backbone is urgently needed.

The modification of the conjugated polymer's side chains is an effective strategy to tune solubility [15–17], absorption spectra [18,19] and electronic energy levels of the conjugated polymers [20–24]. Alkylthio groups have shown a good effect on improving the efficiency of PSCs [25–30]. In addition, the S atom has the ability to accept π electrons from the p-orbital of the C=C double bond to its empty 3 d orbitals. Thus, alkylthio groups can lower the highest occupied molecular orbital (HOMO) of polymer donors to enhance the open-circuit voltage (V_{oc}) of PSCs. For instance, Li et al. has introduced alkylthio substituents into thiophene side chains of the BDT unit, and demonstrated that the introducing of an alkylthio side chain could broaden the absorption and down-shift the HOMO energy level of the low band gap (LBG) 2D-conjunction polymers [31]. Hou et al. has developed a conjugated polymer with a dialkylthio-thienyl substituted benzodithiophene as donor moiety, the open-circuit voltage (V_{OC}) of this polymer is 0.15 V higher than the alkyl-substituted counterpart and the power conversion efficiency (PCE) is thus enhanced [32].

In order to obtain a good performance in PSCs, π-conjugated polymers with good planarity leading to high charge carrier mobility are essential. In general, there are two design strategies to obtain π-conjugated polymers with high planarity. One strategy is to connect neighboring aromatic rings directly through covalent bonds, which

* Corresponding author.
** Corresponding author.
E-mail addresses: wensg@qibebt.ac.cn (S. Wen), zycq@scnu.edu.cn (Y. Zhang).

https://doi.org/10.1016/j.orgel.2019.01.051
Received 13 May 2018; Received in revised form 26 November 2018; Accepted 30 January 2019
Available online 31 January 2019

usually requires a complicated sequence of synthetic steps [33,34]. A more convenient strategy is locking the rotation of single bond by noncovalent interaction such as O···S [35–37], S···S [38–41], N···S [42,43], X···S (X = halide) [44–46]. The S···S noncovalent interaction has been proved to be existent and is applied to induce diverse molecular aggregation. For example, Wang's group revealed the existence of intermolecular S···S interaction by using a high resolution scanning tunneling microscopy (STM) to investigate the molecular packing structures, and demonstrated that intermolecular S···S interaction is vital to direct the 2D self-assembly of a fused thiophene derivative TDT [40]. In addition, Bo's group introduced the alkylthio group to benzothiadiazole-quaterthiophene based conjugated polymers and proved that the introduction of alkylthio substituents can increase the planarity of conjugated polymers [25].

In order to further investigate the effect of the alkylthio side chain on the molecular aggregation and the energy level, we have incorporated an alkylthio-group to a thiophene unit as π bridge to construct a planar conjugated polymer. The alkyl-substituted polymer P1 and the alkylthio-substituted polymer P2 were synthesized to investigate the influence of the alkylthio-substituent on polymer's optoelectronic properties and photovoltaic performance. Compared with P1, the polymer P2 with an alkylthio substituent shows stronger intermolecular interaction, wider absorption range and a higher HOMO energy level. As a result, a higher PCE of 6.15% is obtained for P2 with a V_{OC} of 0.71 V, a short-circuit current (J_{SC}) of 14.55 mA cm^{-2} and a fill factor (FF) of 59.5%.

2. Result and discussion

2.1. Synthesis

The synthetic routes towards P1 and P2 are shown in Scheme 1 and the detailed synthetic procedures are described in the Supporting Information. The polymers P1 and P2 were synthesized through the Stille coupling reaction with $Pd(PPh_3)_4$ as catalyst under argon protection, as shown in Scheme 1. The polymer P1 was purified by Soxhlet extraction with acetone, petroleum ether (PE) and chlorobenzene (CB) in succession, while polymer P2 was extracted with *o*-dichlorobenzene (*o*-DCB) at the final extraction step. P1 shows good solubility in common solvents such as chloroform (CF), tetrahydrofuran (THF), chlorobenzene (CB) et al., while P2 just shows limited solubility in these solvents at room temperature and it is readily soluble only in hot chlorobenzene. The molecular weight of the polymers was estimated by gel-permeation chromatography (GPC) with THF as the eluent. The number average molecular weights (M_n) of polymers were found to be 21.8 kg mol^{-1} with a polydispersity index (PDI) of 1.99 for P1, and 26.3 kg mol^{-1} with a PDI of 2.13 for P2, respectively. As shown in Fig. S1, thermogravimetric analysis (TGA) was used to evaluate the thermal stability of the polymers, and the thermal decomposition temperature (T_d) at 5% weight loss of these two polymers are at 347 °C and 336 °C, respectively. Obviously, these two polymers have good thermal stability, which is adequate for their applications in PSCs devices.

2.2. Optical and electronic properties

The chemical structures of P1 and P2 are plotted in Fig. 1(a) and (b). The normalized UV–vis absorption spectra of the corresponding polymers in solutions and films are shown in Fig. 1(c) and the detailed absorption properties including absorption maxima in solutions and films, as well as absorption onset and bandgaps in the films are summarized in Table 1. As shown in Fig. 1(c), the P1 film shows an absorption band ranging from 450 nm to 736 nm with a λ_{max} at 607 nm, while the absorption band of P2 film is ranging from 550 nm to 771 nm with maxima peaks at 690 nm and 647 nm. The optical bandgap (E_g^{opt}) of P1 and P2 is determined to be 1.68 and 1.61 eV according to the equation: $E_g^{opt} = 1240/\lambda_{onset}$. Compared with P1, P2 shows a red-shifted peak maximum and an obvious shoulder (at 690 nm) in the film spectra, indicating that there should be strong inter-chain aggregation. To make clear the aggregation behavior of these two polymers, the temperature-dependent absorption spectra of P1 (Fig. 1(e)) and P2 (Fig. 1(f)) in dilute *o*-DCB (10^{-5} M) solution were recorded. With the increasing of temperature, the shoulder peak is gradually weakened, accompanied with a blue-shift of several nanometers for the main absorption at 647 nm in dilute P2 solution. The results demonstrate the existence of strong intermolecular stacking, which might be induced by the better planarity better formed in the polymer P2. Cyclic voltammetry tests were employed to evaluate the electrochemical properties of the polymers (Fig. 1(d)). Therefore, P1 and P2 were spin coated on a gold electrode and the measurements were performed in an acetonitrile solution of 0.1 mol L^{-1} Bu_4NPF_6 using ferrocene/ferrocenium (Fc/Fc^+) as the internal standard. The formal potential of Fc/Fc^+ was measured as 0.47 V vs. SCE. From the onset potential for oxidation (E_{ox}), the HOMO energy levels were determined to be −5.74 and −5.28 eV for P1 and P2, respectively. The corresponding lowest unoccupied molecular orbital (LUMO) energy levels were determined to be −4.04 and −3.67 eV, respectively, by the equation $E_{LUMO} = E_{HOMO} + E_g^{opt}$. The steric hindrance of -CH_2 in the hexyl side chain is larger than that of the sulfur atom in the alkylthio side chain. In addition, the sulfur atom in

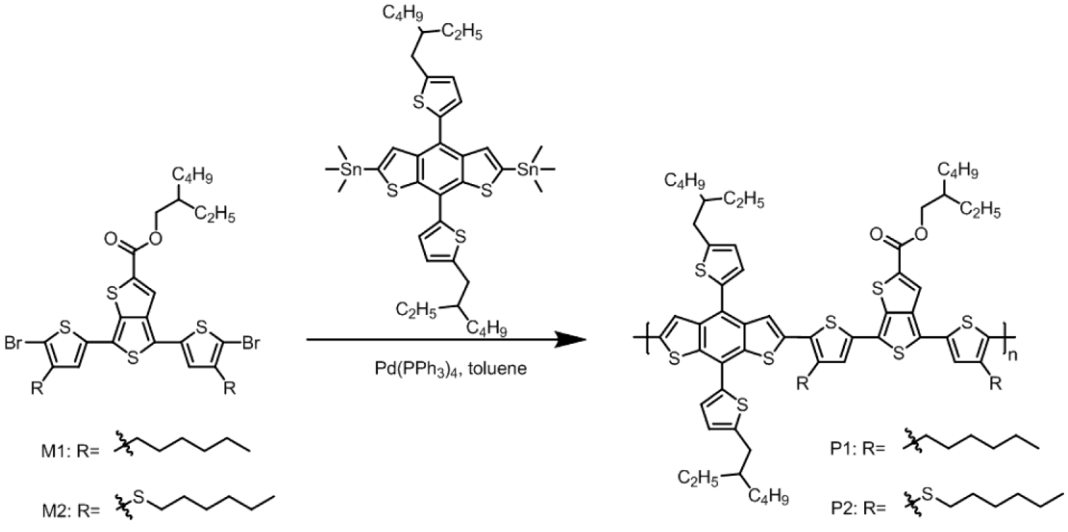

Scheme 1. Synthetic routes of the polymers.

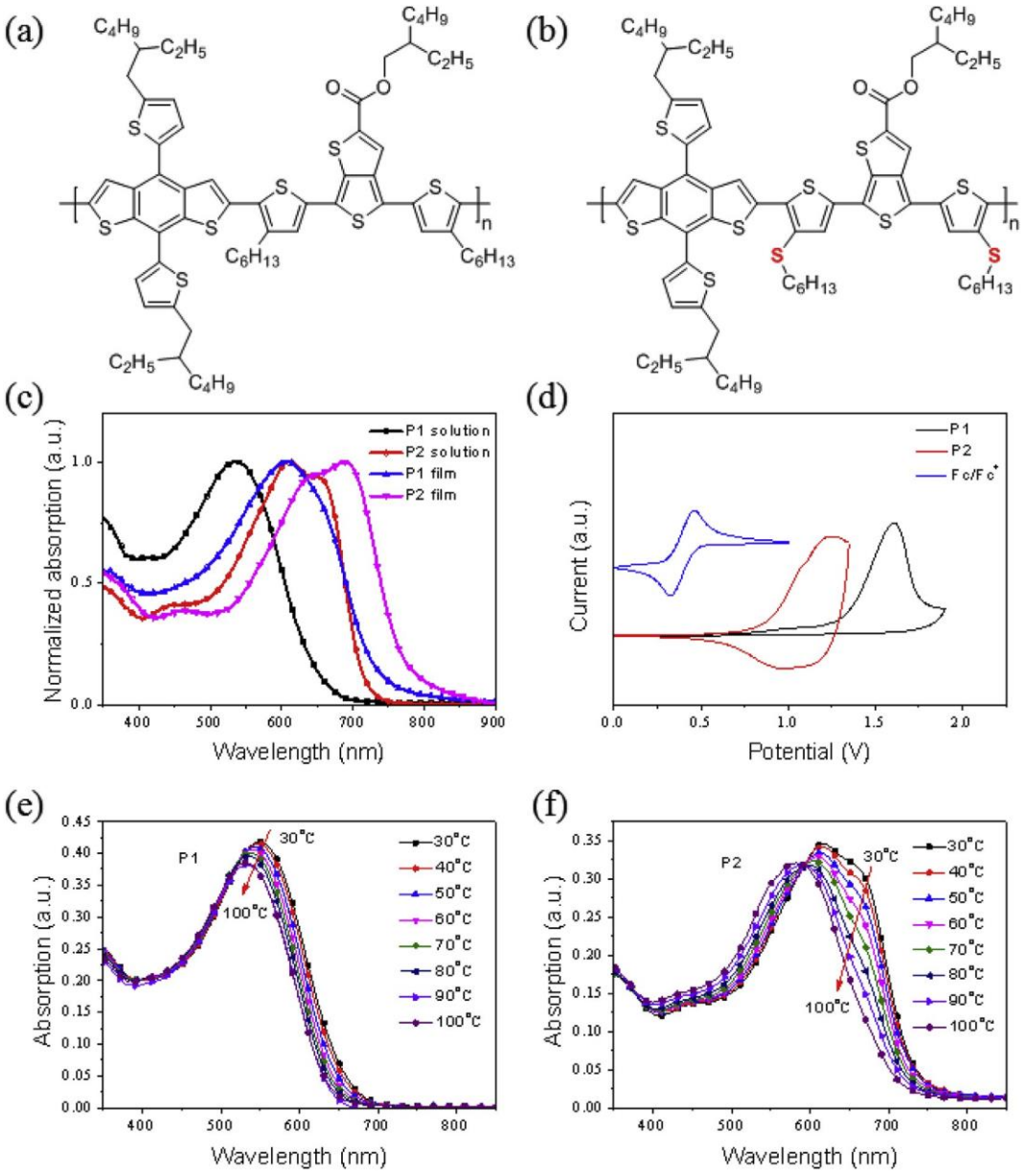

Fig. 1. Chemical structures of P1 (a) and P2 (b). Normalized absorption spectra of P1 and P2 in o-DCB solutions and thin film (c). CV plots of P1 and P2 in thin films (d). Temperature-dependent absorption spectra of P1 (e) and P2 (f) in o-DCB solution.

Table 1
Optical and electrochemical properties of P1 and P2.

Polymer	M_n (kg mol^{-1})	PDI	$\lambda_{sol\text{-}max}$ (nm)	$\lambda_{film\text{-}max}$ (nm)	λ_{onset} (nm)	E_g^{opt}(eV)	HOMO[a] (eV)	LUMO[b] (eV)
P1	21.8	1.99	537	607	736	1.68	−5.74	−4.04
P2	26.3	2.13	611, 650	647, 690	771	1.61	−5.28	−3.67

[a] Estimated from the onset of the oxidation potential.
[b] Calculated by the equation $E_{LUMO} = E_{HOMO} + E_g^{opt}$ (eV).

the alkylthio side chain can form a noncovalent interaction with an adjacent thiophene to maintain the planarity of the molecule. These two reasons make the polymer backbone of P1 more distorted than that of P2. Furthermore, it is reported that the twisting of quinoid type polymer backbones can lower the HOMO energy level [47,48]. Thus, the HOMO of P1 is lower than P2, which can be ascribed to the more distorted polymer backbone of P1.

2.3. Photovoltaic properties

To evaluate the photovoltaic performance of these two polymers, thin film bulk heterojunction solar cells with a conventional device structure of ITO/PEDOT:PSS/polymer:$PC_{71}BM$/PFN/Al were fabricated and characterized. The active layers of the devices were spin-coated from solutions of the polymer donor and the fullerene acceptor, and devices with different blend ratios of the polymer to $PC_{71}BM$ were fabricated to optimize the D/A ratio.

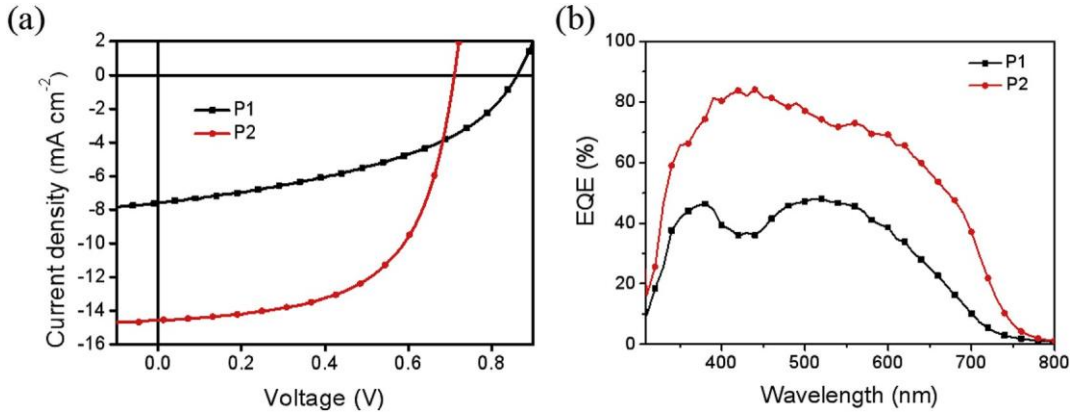

Fig. 2. J-V curves (a) and EQE spectra (b) of the PSC devices prepared with P1 or P2: $PC_{71}BM$ blend with weight ratio of 1:1.5.

Table 2
Photovoltaic parameters of PSCs under illumination of AM 1.5G, 100 mW cm^{-2}.

Polymer/$PC_{71}BM$	D/A ratio	V_{OC} (V)	J_{SC} (mA cm^{-2})	FF (%)	PCE (%)
P1	1:1.5	0.86	7.58	43.4	2.83
P2	1:1.5	0.71	14.55	59.5	6.15

For comparison, the current density-voltage (J-V) curves of the optimized devices are shown in Fig. 2(a) and the corresponding device parameters are summarized in Table 2. The device based on P1 exhibited a PCE of 2.83% with a V_{OC} of 0.86 V, a J_{SC} of 7.58 mA/cm^2, and a FF of 43.4%, while the PSC based on P2 revealed a PCE of 6.15% with a V_{OC} of 0.71 V, a J_{SC} of 14.55 mA cm^{-2} and a FF of 59.5%. It can be observed that the device based on P2 shows higher PCE than that of P1 with a higher J_{SC} and FF, but lower V_{OC} values. The higher V_{OC} of the P1-based device could be attributed to the deeper HOMO level induced

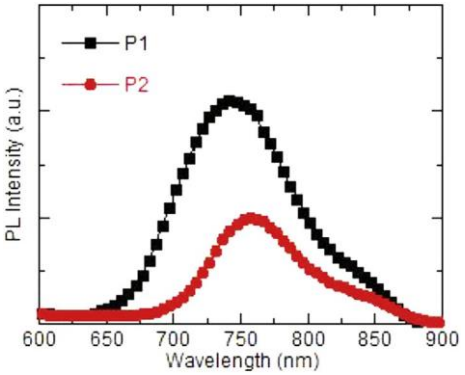

Fig. 4. Photoluminescence spectra of P1:$PC_{71}BM$ and P2:$PC_{71}BM$ blend films.

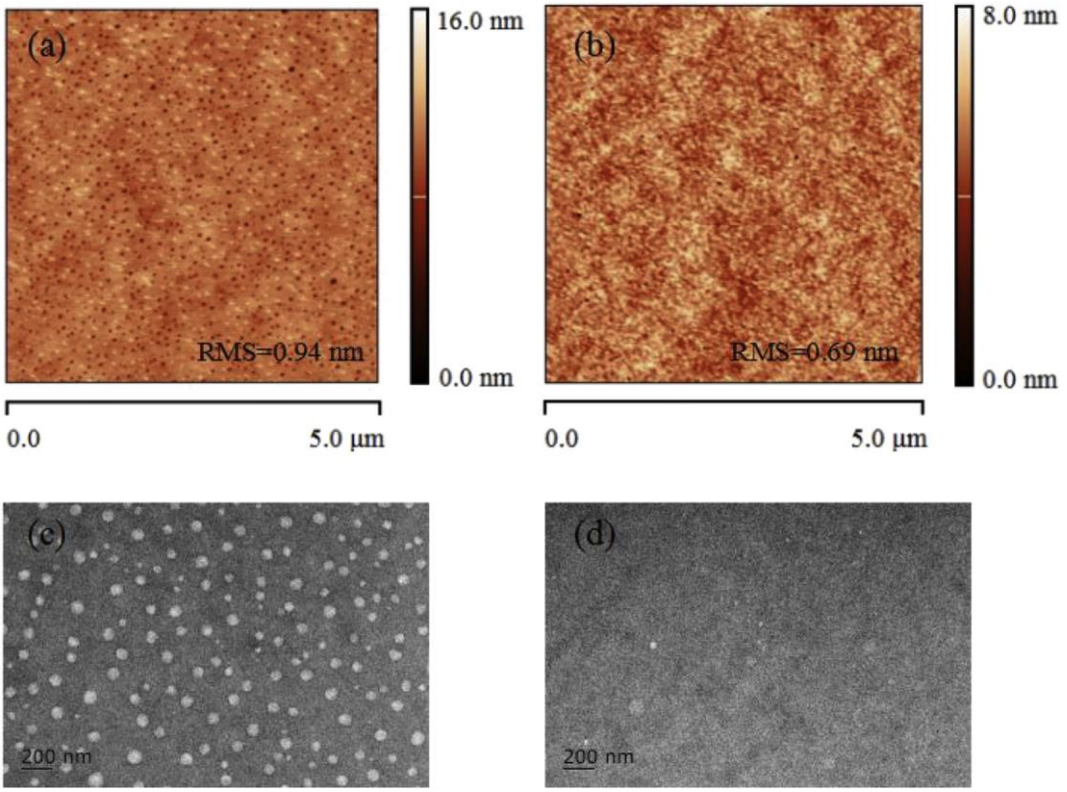

Fig. 3. AFM topography images of P1:$PC_{71}BM$ (a) and P2:$PC_{71}BM$ (b) blend films; TEM images of the corresponding blend films (c, d).

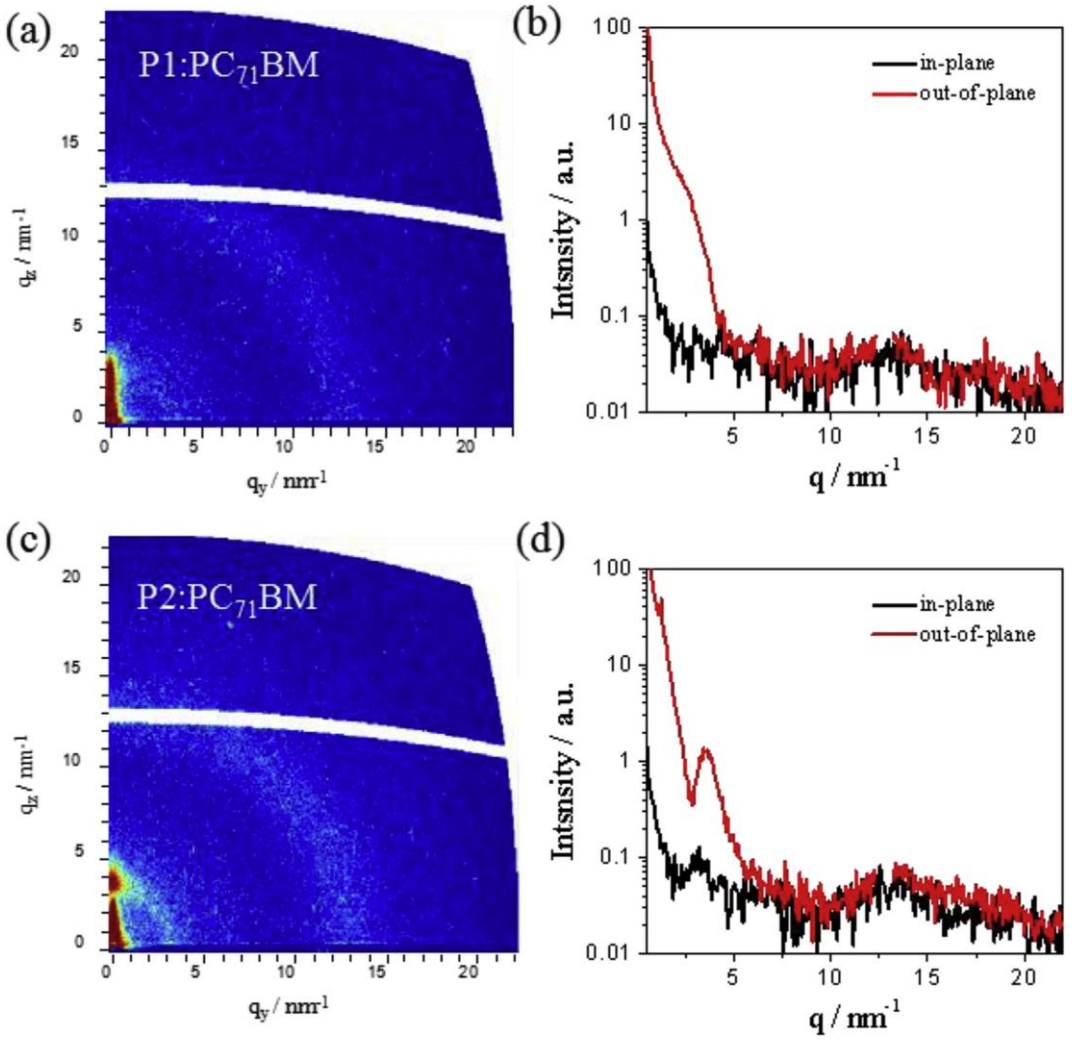

Fig. 5. 2D-GIWAXS images of P1:$PC_{71}BM$ (a) and P2:$PC_{71}BM$ (c) blend films and the corresponding in-plane and out-of-plane GIWAXS profiles (b, d).

by the twisted polymer backbone, which is caused by the larger steric hindrance of the hexyl side chains on the π bridges. The result is in accordance with the energy levels difference observed from cyclic voltammetry. In order to further investigate the photovoltaic performance, space-charge-limited current (SCLC) measurements were performed to study the hole mobility of the polymer and fullerene blend films. The J-V curves of hole-only devices of ITO/PEDOT:PSS/polymer:$PC_{71}BM$/MoO_3/Al are shown in Fig. S2. The hole mobility of P1 blend was determined to be $1.85 \times 10^{-5} cm^2 V^{-1} s^{-1}$, which is one order of magnitude lower than that of the P2 blend (2.20×10^{-4} $cm^2V^{-1}s^{-1}$). The significantly lower hole mobility could be an intrinsic reason for the lower J_{SC} observed in the P1:$PC_{71}BM$ device. External quantum efficiency (EQE) spectra of the optimized devices based on these two polymers are shown in Fig. 2 (b). It can be observed that the P1-based devices exhibit a photo-response from 350 to 700 nm while the photocurrent generation of the P2-based solar cell is extended to higher wavelengths, which is in line with the absorption properties of P1 and P2 (see Fig. 1(a)). The EQE values of the P2:$PC_{71}BM$ device are higher than these of the P1-based device, which is in accordance with the J_{SC} results. The J_{SC}-values calculated from the integration of the EQE data are consistent with the measured J_{SC} values, indicating the reliability of the photovoltaic results.

2.4. Morphology

To further investigate the micromorphology of the P1 and P2 blend films, the morphology of the films based on the optimized conditions was investigated by AFM and TEM, and the images are shown in Fig. 3. The root-mean-square (RMS) roughness is 0.94 nm for the P1: $PC_{71}BM$ blend film and 0.69 nm for the P2: $PC_{71}BM$ blend film. In the TEM images, it can be clearly observed that substantial numbers of holes existed in the P1: $PC_{71}BM$ blend film, which is consistent with the pinhole in the AFM image of the P1: $PC_{71}BM$ blend film, indicating the inferior film-forming ability of the P1: $PC_{71}BM$ blend film. It might be the major cause of low FF in P1 based devices. For the blend film of P2: $PC_{71}BM$, the TEM image shows a smooth morphology, which indicates better miscibility and film-forming property.

The better miscibility of P2 and $PC_{71}BM$ is helpful for charge dissociation and transport in PSCs. In order to verify this, the photoluminescence (PL) quenching measurement was used to explore the effect of alkylthio substituents on the conjugated polymers for exciton dissociation and charge generation. Fig. 4 shows the PL intensity of the P1:$PC_{71}BM$ and P2:$PC_{71}BM$ blend films at an excitation wavelength of 550 nm. The PL intensity of P2:$PC_{71}BM$ blend film is obviously lower than P1:$PC_{71}BM$, suggesting more efficient exciton dissociation and charge generation, which was in accord with the higher short-circuit current observed for the P2:$PC_{71}BM$ blend system. In addition, the emission peak of P2:$PC_{71}BM$ displays a bit red-shift than P1:$PC_{71}BM$, which is consistent with the better molecular planarity due to the S···S non-covalent interaction with an adjacent thiophene.

Detailed nanostructures related to molecular packing in the polymer:$PC_{71}BM$ blend films were also characterized by grazing

incidence wide-angle X-ray scattering (GIWAXS, Fig. 5). By comparing both 2D q-plots in Fig. 5, it can be stated that the P1-blend is presented in an amorphous state due to the lack of obvious diffraction features induced by the distortion of the polymer backbone. Comparatively, the 2D q-plot of the P2-blend reveals the presence of an oriented diffraction peak in the q_z direction (out-of-plane) indicating enhanced ordering in terms of molecular packing parallel to the substrate surface compared to P1. This peak can be interpreted as lamellar scattering which indicates the preferred edge-on orientation of the polymer backbone, testifying that the introduction of the alkylthio group to π-bridge leads to an enhanced intermolecular interaction. This lamellar scattering peak is also visible as slight ring in the 2D q-plot smearing into the q_y direction (peak in the in-plane-cut of P2). The presence of this peak in q_y can be interpreted as randomly distributed species which exhibit no preferential orientation with respect to the substrate. The interlamellar distance was found to be 1.97 nm ($q = 3.18\ \mathrm{nm}^{-1}$) for polymer P2 in the blend films. In both blend films, a broad ring (no preferential orientation) is visible around $q = 12.5 \pm 2.5\ \mathrm{nm}^{-1}$ ($d_{Bragg} = 5.0 \pm 1.0$ Å) which indicates either weak intermolecular vander-Waals interactions in the polymers or can be attributed to short range order in the $PC_{71}BM$ phase of the polymer:$PC_{71}BM$ blend films [49].

3. Conclusion

In summary, two polymers P1 and P2 based on BDT and TT with alkyl and alkylthio side chains on π-bridges were designed and synthesized. Attributed to the less steric hindrance of the alkylthio side chain and thus to a better molecular planarity, the polymer P2 showed a lower E_g^{opt} of 1.61 eV with a HOMO energy level of −5.28 eV. For the optimized P1-based device, a V_{OC} of 0.86 V, a J_{SC} of 7.58 mA cm^{-2} and a FF of 43.4% were obtained, resulting in a PCE of 2.83%. Contributed by the better molecular planarity, P2 exhibited a higher hole mobility of $2.20 \times 10^{-4}\ cm^2V^{-1}s^{-1}$ and an enhanced intermolecular interaction. The optimized P2-based solar cell exhibited a higher J_{SC} of 14.55 mA cm^{-2}, a FF of 59.5%, and a PCE of 6.15%. Our results have demonstrated that alkylthio substitution could be a promising substitution for high efficiency PSCs with excellent planarity.

Acknowledgements

This work was supported by the National Natural Science Foundation of China (No. 61377065 and 61574064), the Ministry of Science and Technology of China (2016YFE0115000), and the Science and Technology Planning Project of Guangdong Province (No. 2013CB040402009, 2015B010132009), the Science and Technology Project of Guangzhou City (No. 2014J4100056, 201607010250). T.R. and G.T. acknowledge financial support by the OEAD S&T Cooperation program (project number CN 01/2016).

Appendix A. Supplementary data

Supplementary data to this article can be found online at https://doi.org/10.1016/j.orgel.2019.01.051.

References

[1] W.C. Zhao, S.Q. Zhang, Y. Zhang, S.S. Li, X.Y. Liu, C. He, Z. Zheng, J.H. Hou, Adv. Mater. 30 (2018) 1704837.
[2] X.P. Xu, T. Yu, Z.Z. Bi, W. Ma, Y. Li, Q. Peng, Adv. Mater. 30 (2018) 1703973.
[3] W. Li, J.L. Cai, F.L. Cai, Y. Yan, H.N. Yi, R.S. Gurney, D. Liu, A. Iraqi, T. Wang, Nano. Energy 44 (2018) 155.
[4] W.C. Zhao, S.S. Li, H.F. Yao, S.Q. Zhang, Y. Zhang, B. Yang, J.H. Hou, J. Am. Chem. Soc. 139 (2017) 7148.
[5] F. Zhao, S. Dai, Y. Wu, Q. Zhang, J. Wang, L. Jiang, Q. Ling, Z. Wei, W. Ma, W. You, C. Wang, X. Zhan, Adv. Mater. 29 (2017) 1700144.
[6] Z. Xiao, X. Jia, L. Ding, Sci. Bull. 62 (2017) 1562.
[7] D. Gao, J. Hollinger, D.S. Seferos, ACS Nano 6 (2012) 7114.
[8] S. Song, K.T. Lee, C.W. Koh, H. Shin, M. Gao, H.Y. Woo, D. Vak, J.Y. Kim, Energy Environ. Sci. 11 (2018) 3248.
[9] J. Kim, S. Park, S. Lee, H. Ahn, S. Joe, B.J. Kim, H.J. Son, Adv. Energy Mater. 8 (2018) 1801601.
[10] G. Yu, J. Gao, J.C. Hummelen, F. Wudl, A.J. Heeger, Science 270 (1995) 1789.
[11] D.Q. Zhu, X.C. Bao, Q.Q. Zhu, C.T. Gu, M. Qiu, S.G. Wen, J.Y. Wang, B.Shahid, R.Q. Yang, Energy Environ. Sci. 10 (2017) 614.
[12] J. Wang, S. Wang, C. Duan, F.J.M. Colberts, J. Mai, X. Liu, X. Jia, X. Lu, R.A.J. Janssen, F. Huang, Y. Cao, Adv. Energy Mater. 7 (2017) 1702033.
[13] C. Duan, K. Gao, F.J.M. Colberts, F. Liu, S.C.J. Meskers, M.M. Wienk, R.A.J. Janssen, Adv. Energy Mater. 7 (2017) 1700519.
[14] L.L. Han, T. Hu, X.C. Bao, M. Qiu, W.F. Shen, M.L. Sun, W.C. Chen, R.Q. Yang, J. Mater. Chem. A 3 (2015) 23587.
[15] J. Kim, C.E. Song, B. Kim, I. Kang, W.S. Shin, D. Hwang, Chem. Mater. 26 (2014) 1234.
[16] E. Wang, L. Hou, Z. Wang, Z. Ma, S. Hellström, W. Zhuang, F. Zhang, O. Inganäs, M.R. Andersson, Macromolecules 44 (2011) 2067.
[17] J. Warnan, C. Cabanetos, R. Bude, A.E. Labban, L. Li, P.M. Beaujuge, Chem. Mater. 26 (2014) 2829.
[18] K. Kawashima, T. Fukuhara, Y. Suda, Y. Suzuki, T. Koganezawa, H. Yoshida, H. Ohkita, I. Osaka, K. Takimiya, J. Am. Chem. Soc. 138 (2016) 10265.
[19] I. Meager, R.S. Ashraf, S. Mollinger, B.C. Schroeder, H. Bronstein, D. Beatrup, M.S. Vezie, T. Kirchartz, A. Salleo, J. Nelson, I. McCulloch, J. Am. Chem. Soc.135 (2013) 11537.
[20] H. Chen, B. Jiang, C. Hsu, Y. Tsai, R. Jeng, C. Chen, K. Wong, Chem. Eur. J. 24 (2018) 1.
[21] T.T. Zhu, D.Y. Liu, K.L. Zhang, Y.H. Li, Z. Liu, X.D. Gao, X.C. Bao, M.L. Sun, R.Q. Yang, J. Mater. Chem. A 6 (2018) 948.
[22] Y.C. Lin, H.W. Cheng, Y.W. Su, B.H. Lin, Y.J. Lu, C.H. Chen, H.C. Chen, Y. Yang, K.H. Wei, Nano. Energy 43 (2018) 138.
[23] T. Kurosawa, X. Gu, K.L. Gu, Y. Zhou, H. Yan, C. Wang, G.-J.N. Wang, M.F. Toney, Z. Bao, Adv. Energy Mater. 8 (2018) 1701552.
[24] Z.H. Luo, Y. Zhao, Z.G. Zhang, G.H. Li, K.L. Wu, D.J. Xie, W. Gao, Y.F. Li, C.L. Yang, ACS Appl. Mater. Interfaces 9 (2017) 34146.
[25] Z. Zhang, Z. Lu, J.C. Zhang, Y.H. Liu, S.Y. Feng, L.L. Wu, R. Hou, X.J. Xu, Z.S. Bo, Org. Electron. 40 (2017) 36.
[26] T. Liu, X. Pan, X. Meng, Y. Liu, D. Wei, W. Ma, L. Huo, X. Sun, T.H. Lee, M. Huang, H. Choi, J.Y. Kim, W.C.H. Choy, Y. Sun, Adv. Mater. 29 (2017) 1604251.
[27] B. Kan, Q. Zhang, M.M. Li, X.J. Wan, W. Ni, G.K. Long, Y.C. Wang, X. Yang, H.R. Feng, Y.S. Chen, J. Am. Chem. Soc. 136 (2014) 15529.
[28] D. Lee, E. Hubijar, G.J.D. Kalaw, J.P. Ferraris, Chem. Mater. 24 (2012) 2534.
[29] Z.C. He, C.M. Zhong, S.J. Su, M. Xu, H.B. Wu, Y. Cao, Nat. Photon. 6 (2012) 591.
[30] D. Lee, S.W. Stone, J.P. Ferraris, Chem. Commun. 47 (2011) 10987.
[31] C. Cui, W.Y. Wong, Y. Li, Energy Environ. Sci. 7 (2014) 2276.
[32] H.F. Yao, H. Zhang, L. Ye, W.C. Zhao, S.Q. Zhang, J.H. Hou, ACS Appl. Mater. Interfaces 8 (2016) 3575.
[33] I. Osaka, S. Shinamura, T. Abe, K. Takimiya, J. Mater. Chem. C 1 (2013) 1297.
[34] B. Liu, L.R. Duan, J.H. Chen, X.W. Duan, T. Lei, Y.F. Cai, Q. Wang, H. Tan, R.Q. Yang, W.G. Zhu, Dyes Pigments 139 (2017) 42.
[35] X.J. Guo, Q.G. Liao, E.F. Manley, Z.S. Wu, Y.L. Wang, W.D. Wang, T.B. Yang, Y. Shin, X. Cheng, Y.Y. Liang, L.X. Chen, K. Baeg, T.J. Marks, X.G. Guo, Chem. Mater. 28 (2016) 2449.
[36] S. Yum, T.K. An, X.W. Wang, W. Lee, M.A. Uddin, Y.J. Kim, T.L. Nguyen, S.H. Xu, S. Hwang, C.E. Park, H.Y. Woo, Chem. Mater. 26 (2014) 2147.
[37] B.Z. Xia, K. Lu, L. Yuan, J.Q. Zhang, L.Y. Zhu, X.W. Zhu, D. Deng, H. Li, Z.X. Wei, Polym. Chem. 7 (2016) 1323.
[38] S. Tsuzuki, H. Orita, N. Sato, J. Chem. Phys. 145 (2016) 174503.
[39] A.G. Flores-Huerta, A. Tkatchenko, M. Galvan, J. Phys. Chem. 120 (2016) 4223.
[40] X.Y. Wang, W. Jiang, T. Chen, H.J. Yan, Z.H. Wang, L.J. Wan, D. Wang, Chem. Commun. 49 (2013) 1829.
[41] F.D. Maria, P. Olivelli, M. Gazzano, A. Zanelli, M. Biasiucci, G. Gigli, D. Gentili, P. D'Angelo, M. Cavallini, G. Barbarella, J. Am. Chem. Soc. 133 (2011) 8654.
[42] Y.Z. Dai, N. Ai, Y. Lu, Y.Q. Zheng, J.H. Dou, K. Shi, T. Lei, J.Y. Wang, J. Pei, Chem. Sci. 7 (2016) 5753.
[43] H. Bronstein, M. Hurhangee, E.C. Fregoso, D. Beatrup, Y.W. Soon, Z.G. Huang, A. Hadipour, P.S. Tuladhar, S. Rossbauer, E. Sohn, S. Shoaee, S.D. Dimitrov, J.M. Frost, R.S. Ashraf, T. Kirchartz, S.E. Watkins, K. Song, T. Anthopoulos, J. Nelson, B.P. Rand, J.R. Durrant, I. McCulloch, Chem. Mater. 25 (2013) 4239.
[44] L. Zhong, L. Gao, H. Bin, Q. Hu, Z.G. Zhang, F. Liu, T.P. Russell, Z.J. Zhang, Y. Li, Adv. Energy Mater. 7 (2017) 1602215.
[45] Z. Zheng, S. Zhang, J. Zhang, Y. Qin, W. Li, R. Yu, Z. Wei, J. Hou, Adv. Mater. 28 (2016) 5133.
[46] J.W. Jo, J.W. Jung, H. Wang, P. Kim, T.P. Russell, W.H. Jo, Chem. Mater. 26 (2014) 4214.
[47] S. Ko, E.T. Hoke, L. Pandey, S. Hong, R. Mondal, C. Risko, Y. Yi, R. Noriega, M.D. McGehee, J. Brédas, A. Salleo, Z.N. Bao, J. Am. Chem. Soc. 134 (2012) 5222.
[48] N. Wang, Z. Chen, W. Wei, Z.H. Jiang, J. Am. Chem. Soc. 135 (2013) 17060.
[49] M. Shao, J.K. Keum, R. Kumar, J. Chen, J.F. Browning, S. Das, W. Chen, J. Hou, C. Do, K.C. Littrell, A. Rondinone, D.B. Geohegan, B.G. Sumpter, K. Xiao, Adv. Funct. Mater. 24 (2014) 6647.